Identification of a MicroRNA-E3 Ubiquitin Ligase Regulatory Network for Hepatocyte Death in Alcohol-Associated Hepatitis

Xiude Fan,[1,2] Jianguo Wu,[1] Kyle L. Poulsen,[1] Adam Kim,[1] Xiaoqin Wu,[1] Emily Huang,[1] Tatsunori Miyata,[1] Carlos Sanz-Garcia,[1] and Laura E. Nagy[1,3,4]

We aimed to identify a microRNA (miRNA)-E3 ubiquitin ligase regulatory network for protein substrates enriched in cell death pathways and investigate the underlying molecular mechanisms in alcohol-associated hepatitis (AH). An miRNA-E3 ubiquitin ligase regulatory network for protein substrates enriched in cell death pathways was constructed using integrated bioinformatics analysis. Differentially expressed hub miRNAs (GSE59492) and their validated miRNA target genes (GSE28619) were identified in the liver of patients with AH compared with healthy controls. Liver samples from patients with AH and healthy individuals and mice exposed to Gao-binge (acute on chronic) ethanol were used for experimental validation. Using hub miRNAs identified by weighted correlation network analysis, a miRNA-E3 ubiquitin ligase regulatory network was established based on 17 miRNAs and 7 E3 ligase genes targeted by these miRNAs that were down-regulated in AH. Among the miRNAs in this regulatory network, miR-150-5p was the only miRNA regulating the E3 ligase cytokine-inducible SH2 containing protein (CISH), the E3 ligase that regulates the largest number of substrates among all E3 ligase family members. Therefore, the CISH regulatory pathway for ubiquitinated substrates was selected for subsequent experimental validation. Consistent with the bioinformatics analysis results, expression of miR-150-5p was markedly increased, while CISH was decreased, in the livers of patients with AH and mice exposed to Gao-binge ethanol. Moreover, ubiquitination of Fas-associated protein with death domain, a predicted CISH substrate involved in the regulation of programmed cell death, was reduced in livers from mice after Gao-binge ethanol. *Conclusion:* Identification of the miRNA-E3 ubiquitin ligase regulatory network for protein substrates enriched in the cell death pathways provides insights into the molecular mechanisms contributing to hepatocyte death in AH. (*Hepatology Communications* 2021;5:830-845).

Alcohol-associated liver disease (ALD) is an important and growing public health problem.[1] ALD progresses from the reversible stages of steatosis, steatohepatitis and fibrosis, to more severe and nonreversible cirrhosis and hepatocellular carcinoma.[2] Clinically, alcohol-associated hepatitis (AH) is a devastating form of ALD, with up to 40% mortality within 90 days.[3] Currently, there are few effective therapeutics available for the treatment of ALD at any stage of disease progression. Therefore,

clarifying the pathogenesis and molecular regulatory pathways involved in ALD is particularly crucial for improving the diagnosis, prevention, and treatment of this disease.

ALD is associated with an increase in hepatocellular death. Multiple forms of programmed cell death, including apoptosis, necroptosis, pyroptosis and ferroptosis, have been implicated in the pathogenesis of ALD.[4-7] Apoptosis and necroptosis, activated by death receptor ligands, have been the most well studied, at least in part because of the important role of tumor necrosis factor (TNF) family members in mediating ALD. Among the ligand-death receptor signaling pathways, the concentration of TNFα, as well as soluble Fas and Fas ligand, are increased in patients with AH.[8,9] Moreover, chronic ethanol exposure shifts TNF receptor 1 (TNFR1) signaling from cell survival to cell death in cultured hepatocytes.[10,11] Fas ligand–induced and TNFR1-induced programmed cell death share many common signaling proteins, including the formation of death-inducing signaling complex by recruiting Fas-associated protein with death domain (FADD), receptor-interacting protein kinase 1 (RIPK1), and caspase-8. Activation of these common pathways is disrupted in liver diseases, resulting in hepatocellular death.[12] However, the regulatory mechanisms by which programmed cell death signaling pathways are dysregulated in ALD is not well understood.

One key mechanism involved in the molecular regulation of death receptor signaling, especially for TNFR1 signaling, is ubiquitination.[13] Ubiquitination of proteins involved in TNFR signaling plays a vital role in determining cell survival or death.[14-16] For example, the cellular inhibitor of apoptosis proteins (c-IAP1 and c-IAP2) act as ubiquitin ligases (E3), catalyzing the poly-ubiquitination of RIPK1 and their own auto-ubiquitination, and regulating the formation of TNFR1 complex I. Because complex I protects against cell death by inhibiting the translocation of RIPK1 to complex II,[14,17] understanding the effect of ethanol on the regulation of ubiquitination could lead to therapeutics to improve hepatocyte survival.

Ubiquitination plays a prominent role in regulating the fate of cellular proteins, affecting their degradation, subcellular localization, and protein–protein interactions. The binding of ubiquitin molecules to target proteins involves two steps: Ubiquitin-activating enzymes (E1) and ubiquitin-conjugating enzymes (E2) prepare ubiquitin for conjugation, and then (2) ubiquitin ligases (E3) link activated ubiquitin to lysine residues of substrates or itself, resulting in protein poly-ubiquitination or mono-ubiquitination.[18] Ligation of ubiquitin to specific lysine residues on target substrates determines the fate of the target protein. For example, poly-ubiquitination through K48-linked ubiquitin chains generally marks proteins for proteasomal degradation, whereas K63-linked ubiquitin chains can regulate signal transduction and tolerance to DNA damage.[18] Previous studies have found that ethanol exposure impairs hepatic proteasome activity,[19-21] due to both changes in the regulation of ubiquitination of proteins and changes in the function of the proteasome.[22] However, the effect of ethanol on the regulation of death receptor signaling by ubiquitination has not been investigated.

ARTICLE INFORMATION:

From the [1]Department of Inflammation and Immunity, Cleveland Clinic, Cleveland, OH, USA; [2]Department of Infectious Diseases, First Affiliated Hospital of Xi'an Jiaotong University, Xi'an, Shaanxi Province, China; [3]Department of Gastroenterology and Hepatology, Cleveland Clinic, Cleveland, OH, USA; [4]Department of Molecular Medicine, Case Western Reserve University, Cleveland, OH, USA.

ADDRESS CORRESPONDENCE AND REPRINT REQUESTS TO:

Laura E. Nagy, Ph.D.
Cleveland Clinic, Lerner Research Institute/NE40
9500 Euclid Ave.
Cleveland OH 44195
E-mail: nagyL3@ccf.org
Tel.: +1-216-444-4021

The regulation of E3 ubiquitin ligases is mediated, in part, by microRNAs (miRNAs). miRNAs are small noncoding RNAs involved in the regulation of gene expression at the post-transcriptional level. Many miRNAs are abnormally expressed in ALD,[23,24] associated with inflammation, hepatocyte death, and hepatocyte regeneration.[23,25] Interestingly, many ubiquitin enzymes, especially the E3 ligases, are regulated by miRNAs, thus affecting the ubiquitination of their target substrates.[26,27] However, the role of miRNAs in the regulation of ubiquitination in ALD has not been investigated. Therefore, in this study, we have identified a miRNA-E3 ligase regulatory network for substrates enriched in programmed cell death pathways using integrated bioinformatics analysis, and then verified this network in liver samples from patients with AH and healthy individuals, as well as in mice exposed to Gao-binge acute-on-chronic model of ethanol-induced liver injury. These analyses identified a miR150-5p cytokine-inducible SH2 containing protein (CISH) network associated with disrupted ubiquitination of FADD, a key protein involved in regulating programmed cell death.

Materials and Methods

MICROARRAY DATA AND PREPROCESSING

Two data sets, GSE59492 and GSE28619, were downloaded from the Gene Expression Omnibus database (https://www.ncbi.nlm.nih.gov/geo/). The miRNA microarray data set GSE59492 was created in the laboratory of Pau Sancho-Bru,[28] using liver samples from 13 patients with AH, 5 with ALD-induced cirrhosis, 5 with nonalcoholic steatohepatitis–induced cirrhosis, 4 with hepatitis C virus–induced cirrhosis, and 6 healthy controls. For our unsigned Weighted Correlation Network Analysis (WGCNA) analysis, we only used the miRNA expression data from the 13 patients with AH and 6 healthy controls. The GSE28619 database contains transcriptome data collected by gene-expression array from livers of 15 patients with AH and 7 healthy controls.[29] Both data sets were preprocessed using R software to transform probes, correct for background, and normalize data distribution. miRNA genes in the GSE59492

data set were analyzed by WCGNA.[30] Differentially expressed genes between AH and normal liver samples in the GSE28619 data set were identified using the limma Bioconductor package.[31]

WGCNA OF miRNA EXPRESSION IN AH

The WGCNA package[30] was used to identify co-expression networks for a total of 1,733 miRNAs in the GSE59492 data set (Fig. 1A). The WGCNA of miRNA expression in AH is described in the Supporting Information.

IDENTIFICATION OF HUB miRNA-TARGET GENES THAT ARE ENRICHED IN THE UBIQUITIN-MEDIATED PROTEOLYSIS PATHWAY

The target genes of the hub miRNAs were identified using miRNet[32] (https://www.mirnet.ca), an integrated tool from three well-annotated and validated miRNA databases: miRTarBase, TarBase, and miRecords. To identify the down-regulated miRNA target genes, a Venn diagram was used to compare the miRNA-target gene set obtained from the miRNet with messenger RNA (mRNA) differentially expressed in the GSE28619 data set. The miRNA-target genes enriched in the ubiquitin-mediated proteolysis pathway were identified using Kyoto Encyclopedia of Genes and Genomes (KEGG) pathway enrichment analysis (Fig. 1B).

IDENTIFICATION OF E3 UBIQUITIN LIGASE–TARGET SUBSTRATES RELATED TO THE APOPTOSIS AND NECROPTOSIS PATHWAYS

The integrated bioinformatics resource UbiBrowser (http://ubibrowser.ncpsb.org) was used to identify the target substrates for E3 ligase. UbiBrowser contains 1,295 validated and 8,255 predicted E3 ligase–substrate interactions. Gene ontology (GO) and KEGG pathway enrichment analysis was performed with Metascape[33] (https://metascape.org) on the identified E3 ligase–target substrates ($P < 0.05$ was the threshold
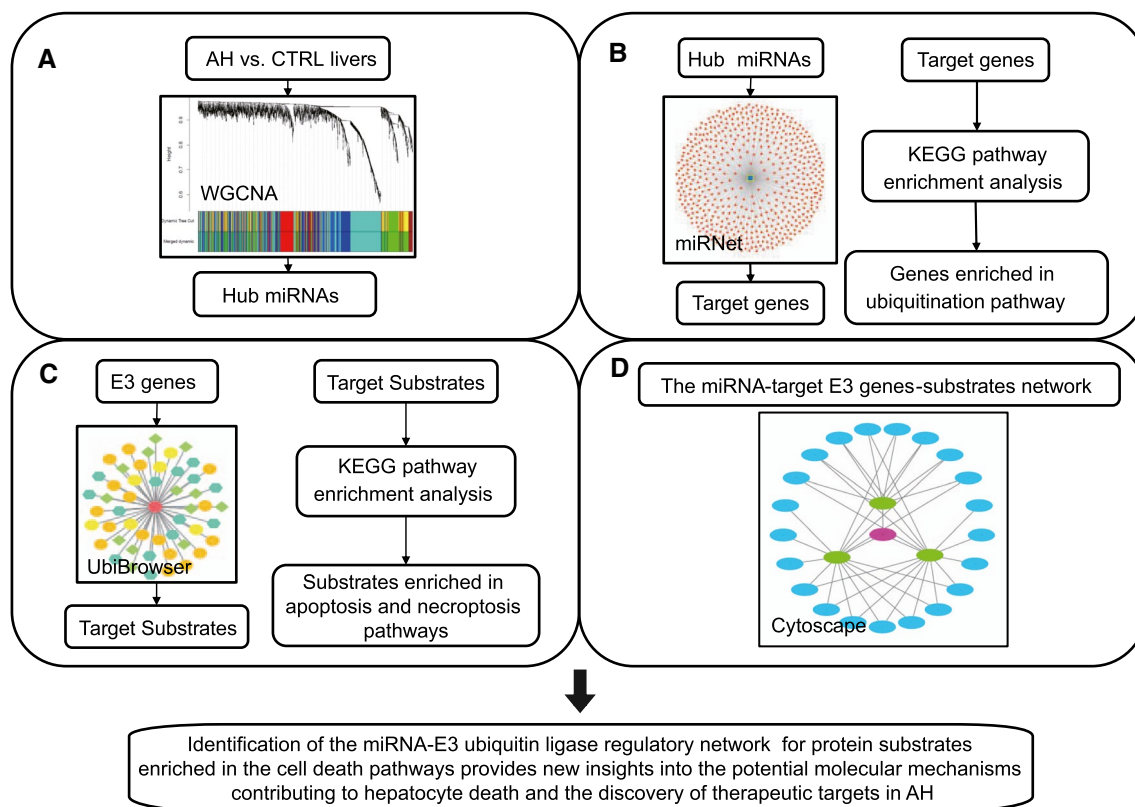
FIG. 1. Schematic overview of bioinformatics methods. (A) Identification of hub miRNAs in AH using WGCNA. (B) MiRNA-target gene prediction based on miRNet and KEGG pathway enrichment analysis to identify miRNA-target genes enriched in ubiquitin-mediated proteolysis pathway. (C) Identification of the E3 ubiquitin ligase–target substrates enriched in the apoptosis and necroptosis pathway using UbiBrowser and Metascape. (D) Construction of the miRNA-E3 ligase gene–substrate regulatory network using Cytoscape.

statistical significance) (Fig. 1C). After KEGG pathway enrichment analysis, the E3 ligase substrates identified as members of the apoptosis (hsa04210) and necroptosis (hsa04217) pathways (Fig. 1C) were selected to construct the miRNA-target E3 substrates network using Cytoscape version 3.7 (Fig. 1D).

CELL CULTURE, miR-150-5p TRANSFECTION, AND LUCIFERASE ASSAY

Alpha mouse liver 12 (AML12) hepatocytes (ATCC, Manassas, VA) were cultured in Dulbecco's modified Eagle's medium/F12 with 10% fetal bovine serum, supplemented with insulin, transferrin, selenium, and dexamethasone. They were seeded in 12-well plates for 24 hours. On the day of transfection, cells were washed and transfected with miR-negative control, miR-150-5p mimic, or miR-150-5p inhibitor

(Qiagen, Hilden, Germany) at 200-nM concentration using RNAiMAX lipofectamine reagent (Thermo Fisher Scientific, Waltham, MA) mixed in the Opti-MEM media as per the manufacturer's instructions. After 48 hours, hepatocytes were lysed for western blot analysis.

The LightSwitch 3′UTR (untranslated region) GoClone containing CISH 3′UTR (insert length = 1,186) was purchased from SwitchGear Genomics (Carlsbad, CA). Twenty-four hours before transfection, 0.014×10^6 cells/well were plated in a 96-well plate. The AML12 cells were then co-transfected with 200 nM miR-150-5p mimic, miR-150-5p inhibitor, or miR-negative control together with the LightSwitch 3′UTR GoClone using RNAiMAX lipofectamine reagent, according to the manufacturer's protocol. After 24 hours, media were removed, cells were lysed with the reagent from the LightSwitch Luciferase Assay Kit (SwitchGear Genomics), and the activity

of luciferase was assayed using the luciferase reporter assay system (SwitchGear Genomics).

PATIENT LIVER SAMPLES

Liver tissues were obtained from the early transplant tissue repository provided by the National Institute on Alcohol Abuse and Alcoholism–supported Clinical Resource for Alcoholic Hepatitis Investigations at Johns Hopkins University (R24AA025017). All liver samples were de-identified and all the studies approved by institutional review boards at Johns Hopkins Medical Institutions and Cleveland Clinic. Biochemical and clinical data for these samples have been reported previously.[34]

GAO-BINGE ETHANOL FEEDING

All animal procedures were approved by the Cleveland Clinic Institutional Animal Care and Use Committee. Female C57BL/6J mice (8-10 weeks old) were purchased from Jackson Laboratory (Bar Harbor, ME). Mice were randomly assigned to ethanol (EtOH)-fed and pair-fed groups. EtOH-fed mice were allowed free access to the Lieber-DeCarli high-fat diet (HFD) containing 5% vol/vol ethanol for 10 days or pair-fed control diets substituting maltose dextrins for ethanol. On day 11, EtOH-fed and pair-fed mice were gavaged with a 5-g/kg dose of EtOH or isocaloric maltose control, respectively. Mice were euthanized 6 hours after gavage. The tissue collection and the feeding protocol have been reported previously.[35]

REVERSE-TRANSCRIPTION AND QUANTITATIVE REAL-TIME POLYMERASE CHAIN REACTION

Total RNA was isolated from human or mouse liver tissue using the Direct-zol mini RNA kit (Zymo Research, Irvine, CA). For miRNA measurement, RNA was reverse-transcribed using the miScript II RT kit (Qiagen). Real-time polymerase chain reaction (PCR) amplification was performed using the miScript SYBR Green PCR kit with miScript primers on a QuantStudio 5 quantitative PCR instrument (Applied Biosystems, Foster City, CA). The mRNA was reverse-transcribed using the Retroscript kit (Invitrogen, Carlsbad, CA). mRNA relative expression was measured using the PowerSYBR quantitative real-time PCR kits (Applied Biosystems). Statistical analyses were performed using the $\Delta\Delta Ct$ method. miRNA was normalized to the small nuclear RNA, RNU6, and mRNA was normalized to 18S rRNA.

IMMUNOBLOTTING, UBIQUITIN ARRAY, AND UBIQUITIN PULL-DOWN ASSAYS

Frozen liver tissues from humans or mice were homogenized in lysis buffer containing protease and phosphatase inhibitors,[35] and protein concentrations assayed using the DC Lowry assay (Bio-Rad, Hercules, CA). N-ethylmaleimide was also added to the lysis buffer for ubiquitin pull-down assays in which 4-mg mouse liver tissue lysate was precleared with control agarose beads (Lifesensors Inc., Malvern, PA) and then pulled down using the Tandem Ubiquitin Binding Entities, agarose-TUBE2 (Lifesensors), which has equivalent affinities for both K63-linked and K48-linked polyUb chains. The Human Ubiquitin Array kit (R&D Systems, Inc., Minneapolis, MN) was used to detect the differences of the ubiquitination levels of proteins between the liver samples from patients with AH and healthy individuals. All experimental operations were performed according to manufacturer's instructions. Liver lysates or ubiquitin pull-down fractions were denatured in Laemmli sodium dodecyl sulfate loading buffer at 95°C for 5 minutes. Then, samples were separated by 10% polyacrylamide gel electrophoresis and subjected to immunoblotting. Antibodies were against CISH (#PA5-79048; Invitrogen), human FADD (#sc-5559; Santa Cruz Biotechnology, Santa Cruz, CA), murine FADD (#sc-6036; Santa Cruz Biotechnology), and HSC70 (#sc-24; Santa Cruz Biotechnology). The densitometry for immunoblots was determined using KODAK Image Station 4000R (Carestream Health, Inc., New York, NY). The relative ubiquitination levels of 49 different proteins in the human ubiquitin array were normalized to the reference spots without overexposure before comparison.

STATISTICS

Continuous variables were represented as the mean and SEM. Two-tailed t tests were used to compare

variables with normal distribution between the two groups. Analysis of variance was conducted using the general linear models procedure. Statistical analyses were performed with STATA (version 16.0; IBM, Armonk, NY) and R (version R-3.6.2). P values < 0.05 were considered significant.

Results

IDENTIFICATION OF HUB miRNAs IN AH USING WGCNA

miRNAs that participate in similar biological process or pathways may be tightly co-regulated and have similar expression patterns.[36] WGCNA was used to identify miRNAs that are closely connected by forming weighted gene co-expression networks (modules) of miRNAs related to AH (Fig. 1). As shown in the sample dendrogram and trait heatmap (Fig. 2A), 1,733 miRNAs were selected from the GSE59492 data set to construct the miRNA co-expression network (Fig. 2B). A total of five miRNAs modules were identified that correlated with AH (Fig. 2C). There were 338 miRNAs in the blue module, 283 miRNAs in the brown module, 408 miRNAs in the green module, 125 miRNAs in the red module, and 579 miRNAs in the turquoise module. Module clinical traits association analysis demonstrated that the blue (cor = –0.88, $P = 8^7$) module was negatively correlated with AH. In contrast, green (cor = 0.69, $P = 0.001$) and turquoise (cor = 0.48, $P = 0.04$) modules were positively correlated with AH (Fig. 2C), indicating that miRNAs in these modules were up-regulated in AH (Supporting Fig. S1). The module eigengenes and clinical trait (AH) hierarchical clustering and heatmap indicated that the green module was highly correlated with AH (Fig. 2D). Finally, gene significance (GS) versus module membership (MM) were plotted for the AH-related green module to identify hub miRNAs that were highly associated with AH (Fig. 2E). These miRNAs are listed in Supporting Table S2. A total of 39 miRNAs with GS > 0.42 and MM > 0.74 were selected to use in the identification of miRNA target genes using miRNet. Importantly, using KEGG pathway enrichment analysis, we found that 30 of these 39 miRNAs had target genes that were identified as enriched in ubiquitin-mediated proteolysis pathway (Fig. 2F).

UBIQUITINATION OF PROTEINS ENRICHED IN THE PROGRAMMED CELL DEATH PATHWAY IN PATIENTS WITH AH

To investigate whether ubiquitination levels of proteins enriched in cell death pathway change in patients with AH, we first used a human ubiquitin array to evaluate the ubiquitination levels of 49 different proteins in the liver samples from 3 patients with AH and 3 healthy individuals (Fig. 3A). Ubiquitination of caspase-8, tumor protein P53, and inhibitor of nuclear factor kappa B kinase regulatory subunit gamma were increased in the liver samples of patients with AH, whereas c-IAP1, c-IAP2, nuclear factor kappa B inhibitor epsilon, and TNF receptor associated factor 6 were decreased in the liver of patients with AH compared with those of healthy individuals (Fig. 3B). Because these proteins were enriched in programmed cell death pathway, the data suggest that ubiquitination of proteins enriched in programmed cell death pathway may be involved in determining cell survival or death during the progression of AH. Therefore, understanding the effect of ethanol on the regulation of ubiquitination could lead to therapeutics, to improve hepatocyte survival).

IDENTIFICATION OF HUB miRNA-TARGET E3 UBIQUITIN LIGASE GENES AND E3 SUBSTRATES ENRICHED IN APOPTOSIS AND NECROPTOSIS PATHWAYS

Because the ubiquitin-mediated proteolysis pathway was identified as important in AH in our *in silico* prediction from the miRNA database, we next asked whether the ubiquitin-mediated proteolysis pathway was also regulated in AH in the GSE28619 transcriptome database. In total, 14 down-regulated E3 ubiquitin ligase genes were identified in the liver samples of patients with AH from the GSE28619 data set (Fig. 4A and Supporting Table S1). These included the catalytic E3 ligases, as well as noncatalytic E3 ligase complex components, which were found to be regulated by hub miRNA in the E3 ligase gene set. The intersection between the down-regulated E3 ligase gene set of GSE28619 and hub miRNA-target E3 ligase gene set (Supporting Table S2) is illustrated in the Venn diagram

(Fig. 4B). Seven E3 ligases (including two noncatalytic E3 ligase complex components) were identified as overlapping in the Venn diagram: CISH, kelch-like family member 15 (KLHL15), siah E3 ubiquitin protein ligase 2 (SIAH2), zinc finger and BTB domain containing 16 (ZBTB16), zinc and ring finger 3 (ZNRF3), zinc finger AN1-type containing 5 (ZFAND5), and zinc finger and BTB domain containing 10 (ZBTB10)

A Sample dendrogram and trait heatmap

B Cluster Dendrogram

C Module–trait relationships

D Eigengene dendrogram and Eigengene adjacency heatmap

E Module membership vs. gene significance

F miRNA-target genes associated with the ubiquitin-mediated proteolysis pathway
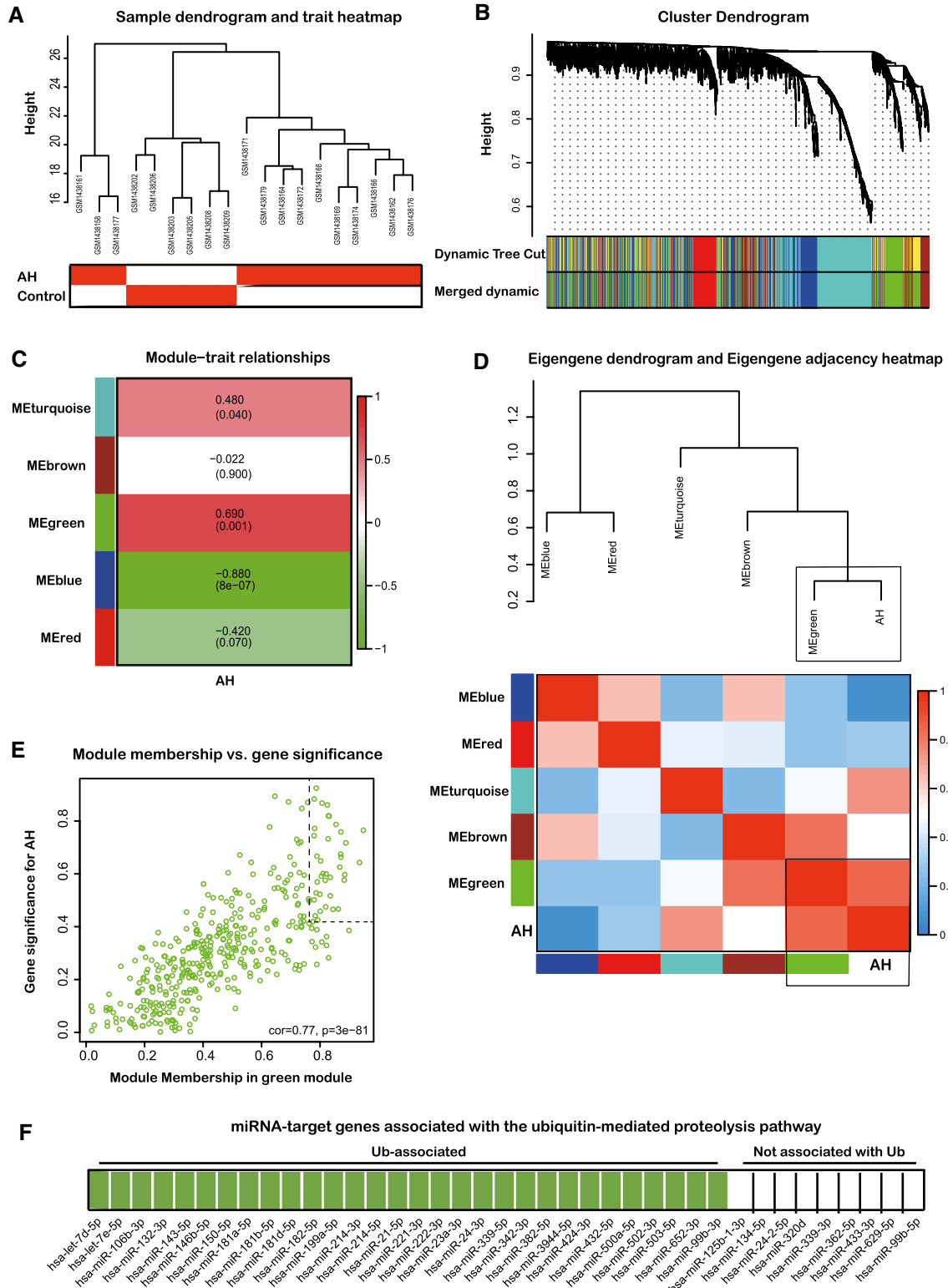
FIG. 2. Hub miRNAs obtained following WGCNA analysis of total miRNAs from the livers of patients with AH and healthy controls in the GSE59492 data set. (A) Sample dendrogram and trait heatmap. The cut height was set as 22, and none of the samples exceeded the cutoff threshold. (B) Hierarchical cluster analysis was conducted to identify miRNA co-expression clusters using the GSE59492 data set. MicroRNAs within five modules were identified and labeled with five colors (turquoise, brown, green, blue, and red). The branches of the dynamic clustering tree correspond to the clusters/modules shown as colored bands underneath the cluster tree. The highly similar miRNA modules were merged and are shown as the merged dynamic colored bands. (C) Heatmap depicts the correlations between modules and clinical trait (AH versus controls). The degree of correlation was represented by different colors (numerical scale on the right-hand side and colors on the left-hand side represent each module). Each row was labeled with correlation coefficients and *P* value. (D) Correlation between module eigengenes and clinical trait (AH), showed by hierarchical clustering and heatmap. The dotted box indicates modules that strongly cluster with AH. (E) Scatter plot between the green module membership and the gene significance for clinical trait (AH). The x-axis represents the module membership in the green module, and the y-axis represents the gene significance in the green module. (F) KEGG pathway enrichment analysis for miRNA-target genes selected from the green module. In total, 30 of the 39 miRNAs target genes in the green module are enriched in the ubiquitin-mediated proteolysis pathway.

(Fig. 4B). As would be expected, when we asked what miRNAs regulate these seven E3 ligase genes, we found that 17 miRNAs from the green module of the GSE59492 data set regulate these E3 ligase genes. The miRNA-target E3 ligase genes in this regulatory network are shown in the Fig. 4C.

IDENTIFICATION OF E3 LIGASE SUBSTRATES

To better understand the biological impact of differences in E3 ligase expression in the liver of patients with AH, UbiBrowser was used to predict protein substrates for the seven E3 ligases identified in our analysis. CISH interacts with 1,012 protein substrates; KLHL15 interacts with 20 protein substrates; SIAH2 interacts with 912 protein substrates; and ZBTB16 interacts with 877 protein substrates. ZNRF3 and the noncatalytic E3 ligase complex components (ZFAND5 and ZBTB10) had no predicted substrates. To determine the function of these E3 ligase–target substrates, KEGG pathway and GO (biological process) enrichment analyses were conducted using Metascape. The top 20 enriched pathways and biological processes identified are shown in Fig. 4D,E. Given the critical role of ubiquitination in the regulation of programmed cell death pathways, functional enrichment analysis was used to identify the E3 ligases in our gene set that were enriched in programmed cell death pathways. Based on this analysis, CISH was selected as having the highest number of target substrates in the apoptosis and necroptosis pathways (Supporting Table S3). Of the 17 miRNAs included in the miRNA-target E3 ligase gene regulatory network (Fig. 4C), we found that miR-150-5p was the only miRNA that regulates CISH. To identify appropriate targets to experimentally validate the regulation of miR150-5p and CISH in AH, we

constructed an miRNA-target E3 ligase gene-substrate network (Fig. 4F). This network includes the miR-150-5p-target E3 ligase gene (CISH) and 66 CISH-target substrates that are enriched in apoptosis and necroptosis pathways. Similar results were obtained using ingenuity pathway analysis (data not shown).

PATIENTS WITH AH AND MICE EXPOSED TO GAO-BINGE ETHANOL HAVE INCREASED EXPRESSION OF Mir-150-5p AND DECREASED EXPRESSION OF CISH IN LIVER

Expression of miR-150-5p was increased in the livers of patients with AH compared to healthy individuals (Fig. 5A). Gao-Binge EtOH feeding in mice is associated with increased liver damage and neutrophil accumulation, a model that has features characteristic of human AH.[34,35] Here we used liver samples from mice exposed to Gao-binge EtOH; these mice were previously shown to have increased hepatic triglycerides, circulating alanine aminotransferase and aspartate aminotransferase, as well as increased accumulation of neutrophils, as assessed by NIMPR14 staining.[37] Expression of miR-150-5p was increased in the livers of EtOH-fed mice compared with pair-fed mice (Fig. 5B). Expression of CISH mRNA and protein was decreased in the livers of patients with AH and EtOH-fed mice compared with healthy individuals (Fig. 5C/E) and pair-fed mice (Fig. 5D/F), respectively. Through computational analysis using STarMirDB,[38] we obtained the nucleotide positions of predicted binding sites of miR-150-5p and 3′UTR-CISH (Fig. 6A). To confirm that CISH is a target of miR-150-5p, we examined the effect of miR-150-5p mimic and inhibitor in AML12 cells, a murine hepatocyte cell line.
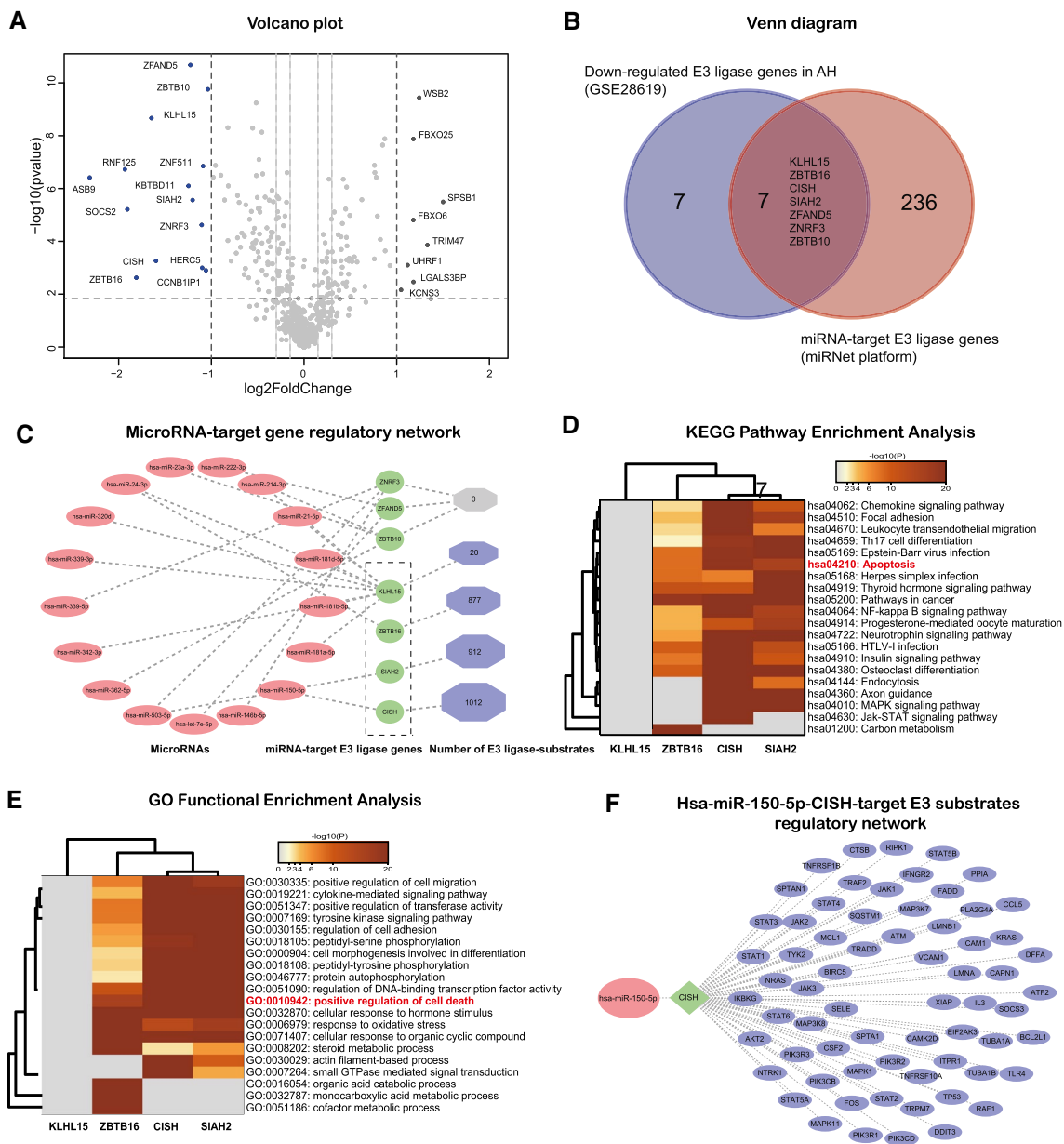
FIG. 3. Ubiquitination of proteins enriched in the programmed cell death pathway in liver samples from patients with AH. (A) The human ubiquitin array kit was used to evaluate the ubiquitination levels of proteins in liver samples from patients with AH and healthy individuals (n = 3 for each group). The framed proteins were detected in all samples. (B) Relative ubiquitination was semi-quantified for all proteins. Proteins identified with an asterisk (*) are proteins enriched in the cell death pathway that were significantly changed in the liver samples of patients with AH compared to those of healthy individuals. Proteins identified with a triangle (△) are proteins whose ubiquitination was very low or undetectable in the ubiquitination screen assay. Data are represented as fold change of AH versus healthy control. Values are presented as means ±SEM, n = 3. Abbreviation; HC, healthy control.

Expression of CISH protein was significantly increased 48 hours after transfection of AML12 hepatocytes with miR-150-5p inhibitor (200 nM) compared with expression in AML12 cells transfected with scrambled small interfering. However, transfection with the miR-150-5p mimic (200 nM) did not reduce CISH protein levels at 48 hours, perhaps due to a slower rate of CISH protein degradation (Fig. 6B). To provide more direct

evidence that miR-150-5p targets CISH, we co-transfected AML12 hepatocytes with a plasmid containing a luciferase gene under the control of CISH 3′UTR and either the miR-150-5p mimic, inhibitor, or miRNA negative control. Luciferase activity increased in cells transfected with miR-150-5p inhibitor and decreased in cells transfected with miR-150-5p mimic compared to cells transfected with the negative control (Fig. 6C).

FIG. 4. Identification of the E3 ubiquitin ligase–target substrates related to the apoptosis and necroptosis pathways. (A) Volcano plot of E3 ubiquitin ligase DEGs between AH and healthy liver samples from the GSE28619 data set. The red points represent up-regulated mRNA screened on the basis of log FC > 1 and adjusted P value of < 0.05. The blue points represent down-regulation of the expression of genes screened on the basis of log FC < –1 and a corrected P value of < 0.05. The gray points represent genes with no significant difference. (B) Venn diagram of the intersection between the E3 ligase differentially expressed gene set of GSE28619 and the hub miRNA-target E3 ligase genes set. Seven E3 ligase genes were identified in the overlap region. (C) MiRNA-target E3 ligase gene regulatory network. This network showed seven E3 ligase genes regulated by 17 miRNAs and the number of these E3 ligase–target substrates from UbiBrowser. (D) KEGG pathway enrichment analysis of E3 ligase–target substrates using Metascape. The top 20 enriched pathways are shown. CISH-target substrates were selected for subsequent studies, as the number of CISH-target substrates enriched in the apoptosis and necroptosis pathway are larger than the other E3 ligase-target substrates. (E) GO enrichment analysis in biological processes for E3 ligase–target substrates. The top 20 enriched biological processes are shown. (F) MiR-150-5p-target E3 ligase gene–substrate network. This network includes miR-150-5p-target E3 ligase gene (CISH) and 66 CISH-target substrates enriched in the apoptosis and necroptosis pathways. This network was obtained with Cytoscape. Abbreviations: DEG, differentially expressed gene; FGFR, fibroblast growth factor receptor 1.
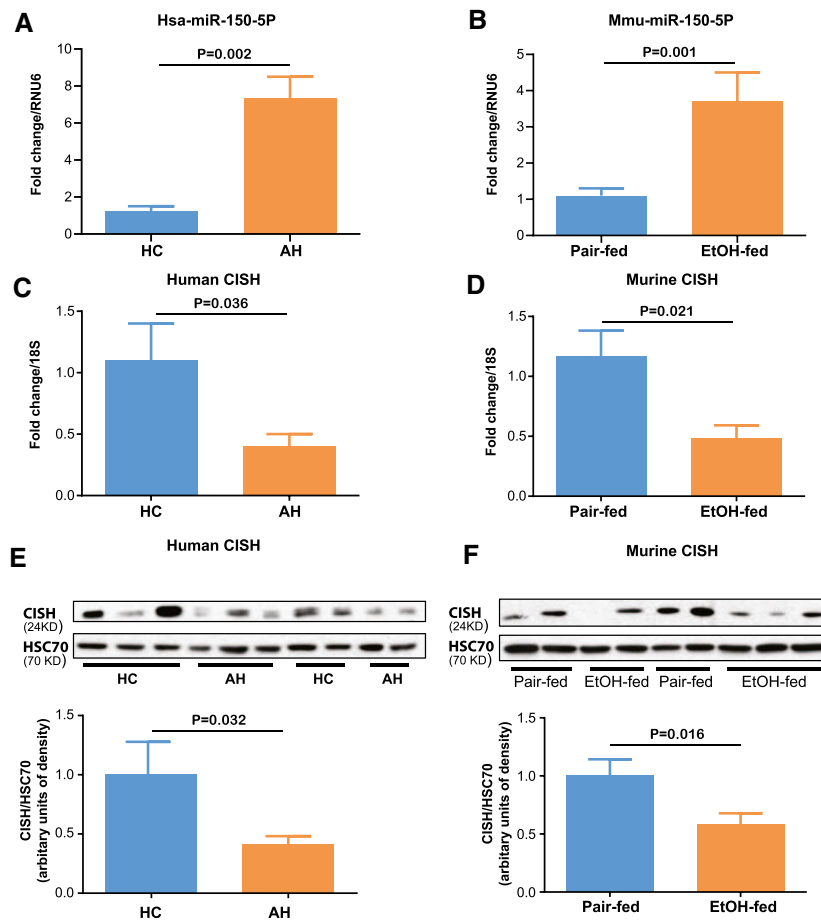
FIG. 5. Increased miR-150-5p and decreased CISH were identified in patients with AH and the Gao-Binge mice model. Expression of miR-150-5p was determined in human livers (A) and mice livers (B) using quantitative real-time PCR and normalized to RNU6. Data are represented as fold change of EtOH versus pair group (n = 5-7 for each group). Expression of CISH was determined in human livers (C) and mice livers (D) using quantitative real-time PCR and normalized to 18 seconds. Data are represented as fold change of EtOH versus pair group (n = 5-7 for each group). (E) Expression of CISH protein was measured in the livers of patients with AH and heathy individuals by western blot (n = 5 for each group). Densitometry was carried out with HSC70 as a loading control. (F) Expression of CISH protein was measured in the livers of mice by western blot (n = 4-5 for each group). Densitometry was carried out with β-actin as a loading control. Values represent means ± SEM, and P values are presented at the top of the bar graphs.

UBIQUITINATION OF THE CISH-TARGET FADD WAS REDUCED IN GAO-BINGE-INDUCED LIVER INJURY, AND FADD EXPRESSION WAS HIGHER IN THE LIVER OF PATIENTS WITH AH AND MICE EXPOSED TO GAO-BINGE EtOH

Because FADD is both a substrate of CISH and a critical component in multiple receptor-mediated cell death pathways,[39] we chose to measure FADD ubiquitination and expression to experimentally confirm our *in silico* analysis. The intersection between down-regulated E3 ligase genes in AH from GSE28619 and the predicted E3 ligases for FADD (Supporting Table S4) is shown in Fig. 5A. CISH was identified from the Venn diagram as the only down-regulated E3 ligase for FADD in AH (Fig. 7A). Consistent with the reduced E3 ligase CISH in AH, the level of ubiquitinated FADD was reduced in the livers of EtOH-fed mice compared with pair-fed mice (Fig. 7B). Furthermore, accumulation of M30, a caspase-3 cleavage product of CK18, was increased in the livers of these EtOH-fed mice compared with pair-fed mice.[37] Furthermore, expression of FADD protein was increased in the livers of patients with
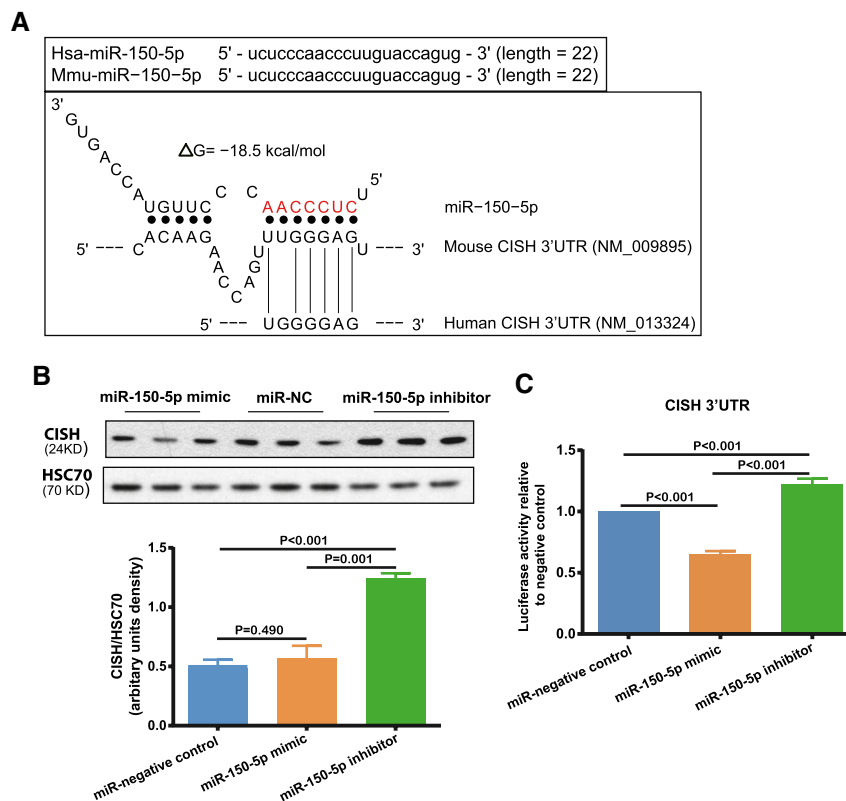
FIG. 6. miR-150-5p directly targets CISH. (A) Predicted target site of miR-150-5p in 3′UTR region of CISH mRNA and sequence alignment between the mouse 3′UTR-CISH and human 3′UTR-CISH by BLAST. The dots represent target sites, and the vertical lines indicate similarity between human and murine sequences. (B) AML12 cells were transiently transfected with miR-150-5p mimic, inhibitor, or miRNA negative control (200 nM) for 48 hours, and protein levels of CISH were determined by western blot (n = 3). (C) The luciferase reporter plasmid containing CISH 3′UTR was co-transfected with miR-150-5p mimic, inhibitor, or miRNA negative control (200 nM) in AML12 cells. Luciferase activities were determined at 24 hours after transfection. The relative luciferase activity was normalized to the miRNA negative control group. Values represent means ± SEM, and *P* values are presented at the top of the bar graphs.

AH and EtOH-fed mice as compared with healthy individuals (Fig. 7C) and pair-fed mice (Fig. 7D), respectively. Previous work, using the same human liver samples, revealed an increase in caspase-3 and caspase-9 cleavage in patients with AH compared to healthy controls.[35]

Discussion

In this study, we constructed a network of miRNAs regulating E3 ubiquitin ligases for substrates enriched in the programmed cell death pathways in AH using bioinformatic analysis, and identified FADD as a critical target of the miR-150-5p-CISH network. This network was experimentally verified in the livers of patients with AH and mice exposed to the Gao-binge model of EtOH-induced liver injury. Overall, our results suggest that changes in the expression of miR-150-5p-target CISH in AH or in response to Gao-binge EtOH feeding reduce the ubiquitination and increase the accumulation of FADD (Fig. 7E) and may act to promote hepatocellular death in AH.

We identified the elevated expression of miR-150-5p in AH. Pre-miR-150 is a miRNA precursor that is processed to two mature forms: miR-150-3p and miR-150-5p. miR-150 is up-regulated in the liver of patients with nonalcoholic fatty liver disease and HFD-fed mice, and is associated with insulin resistance and hepatic steatosis through regulation of FADD-like apoptosis regulator.[40] Moreover, deletion of miR-150 prevents Fas-induced liver injury and hepatocyte apoptosis through the regulation of the protein kinase B pathway, but not lipopolysaccharide-induced
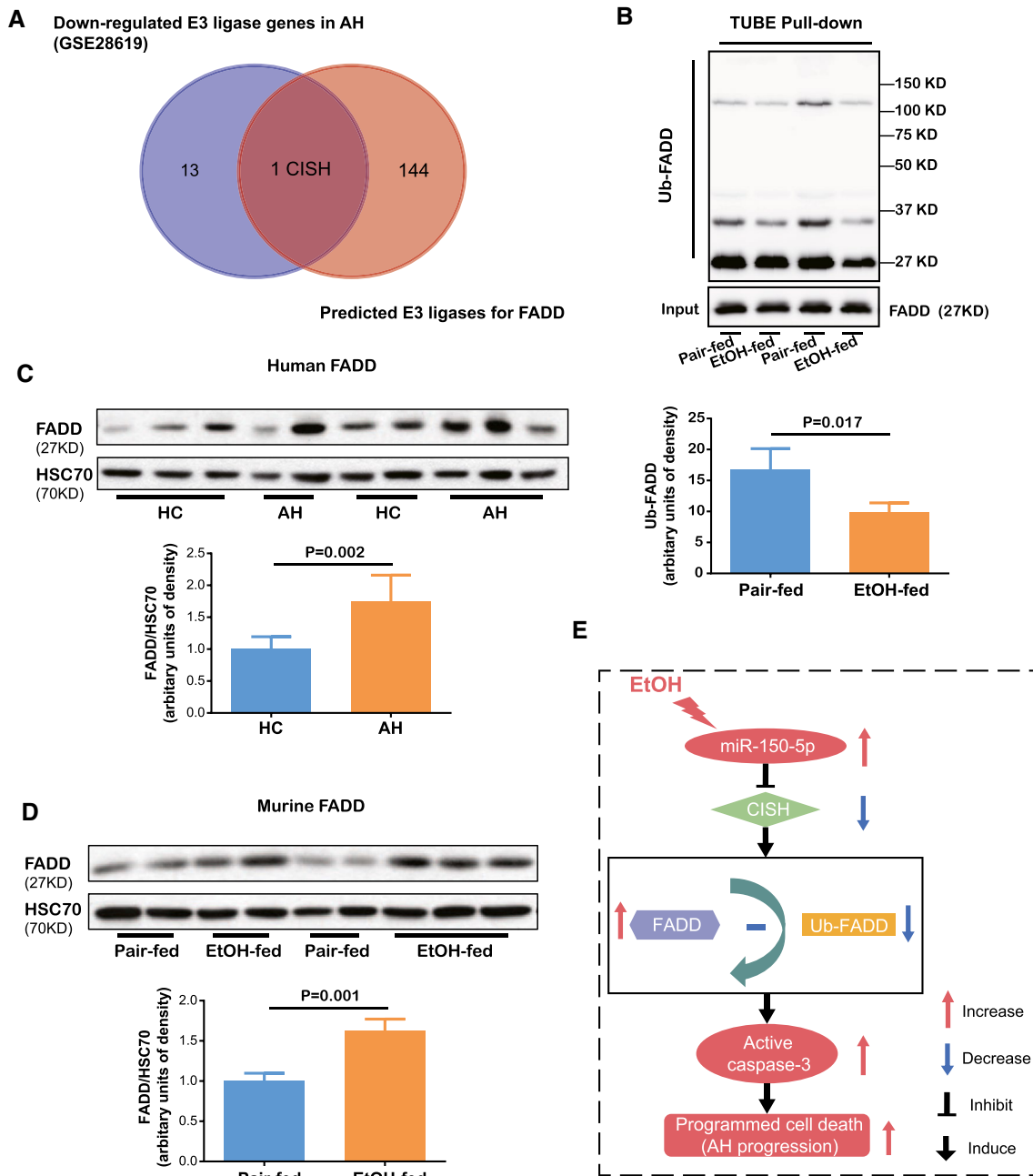
FIG. 7. Ubiquitination levels of CISH-target FADD were reduced in the Gao-Binge mice model of EtOH-induced liver injury. (A) Venn diagram of the intersection between down-regulated E3 ligase genes of GSE28619 and predicted E3 ligase genes for FADD. Only CISH was identified in the overlap region. (B) FADD ubiquitination in mouse livers was measured by TUBE pull-down assays, which enriched ubiquitinated proteins. The pull-down fractions were resolved in sodium dodecyl sulfate–polyacrylamide gel electrophoresis and examined in immunoblotting with anti-FADD antibody. Bands above FADD (27 KD) represent Ub-FADD with higher molecular weight. Pull-downs are representative of 4-5 mice per diet group. (C) Expression of FADD protein was measured in the livers of patients with AH and heathy individuals by western blot (n = 5 for each group). Densitometry was carried out with HSC70 as a loading control. (D) Expression of FADD protein was measured in the livers of mice by western blot (n = 4-5 for each group). Densitometry was carried out with β-actin as a loading control. Values represent means ± SEM, and *P* values are presented at the top of the bar graphs. (E) Overview of the potential network of miR-150-5p-CISH-FADD in EtOH-induced hepatocyte death. Changes in the expression of miR-150-5p-target CISH in AH or in response to Gao-binge EtOH feeding reduce the ubiquitination and increase the accumulation of FADD, which may lead to increased caspase-3 activation and cell death.

liver injury.[41] Expression of hepatic miR-150-5p is increased in CCl$_4$-induced liver fibrosis in mice,[42] particularly in apoptotic hepatocytes, but not activated hepatic stellate cells (HSCs), and is involved in the progression of hepatic fibrosis.[42,43] Here we find that expression of miR-150-5p was increased in the livers of patients with AH and mice after Gao-Binge EtOH exposure, suggesting that miR-150-5p may be involved in the pathogenesis of ALD.

To establish the miRNAs-E3 ubiquitin ligases regulatory network, we identified CISH as an important miRNAs-regulated E3 ligase gene using the validated miRNA databases.[32] Previous work confirmed that the expression of CISH mRNA is decreased in HSCs when transfected with miR-150-5p mimics.[42] Here we used a luciferase reporter assay to confirm that expression of CISH was directly regulated by miR-150-5p by binding to the 3′UTR of CISH. In addition, we found that hsa-miR-150-5p regulates 38 target genes, verified by luciferase reporter assays in previous studies.[32] Of these, only two additional target genes, early growth response 2 (EGR2; logFC = –2.92, adjusted P < 0.05) and vascular endothelial growth factor A (VEGFA; logFC = –0.97, adjusted P < 0.05), were found to be significantly reduced in the livers of patients with AH compared to healthy controls in the GSE28619 data set. Because previous studies have found that both EGR2[44] and VEGFA[45] are involved in the regulation of programmed cell death, suggesting that, in addition to the miRNAs-E3 ligase regulatory network characterized here, additional miRNAs regulatory pathways regulating programmed cell death may also exist.

CISH is a member of the suppressor of cytokine signaling (SOCS) family[46] and functions to suppress cytokine signaling by inhibiting the Janus kinase–signal transducer and activator of transcription 5 pathway.[46,47] In addition, CISH is a substrate-recognition component of the elongin B/C-Cul2/Cul5-SOCS box protein (ECS) E3 ubiquitin ligase complex, which regulates the ubiquitination of target substrates.[47] In total, 66 CISH-target substrates enriched in the apoptosis and necroptosis pathway were identified using UbiBrowser and KEGG pathway enrichment analysis, indicating that it is an important nexus for the regulation of cell death pathways.

Among the substrates targeted by CISH, FADD is a key protein that bridges multiple death receptor signaling to the caspase-dependent signaling cascade by forming a death-inducing signaling complex with procaspase-8, which is essential for the induction of extrinsic apoptotic cell death.[39] As the direct adaptor for both the Fas and TNF-related apoptosis-inducing ligand (TRAIL) receptors, FADD deficiency abolishes Fas-induced and TRAIL receptor–induced cell death.[39,48] Furthermore, miR-150 deficiency also has been reported to prevent Fas-induced hepatocyte apoptosis,[41] and miR-150-5p is up-regulated in apoptotic hepatocytes.[42] Importantly, CISH was identified as the only down-regulated E3 ligase that targets FADD in the liver of patients with AH. Thus, we hypothesized that miR-150-5p may affect the ubiquitination degradation of FADD by inhibiting CISH expression. Consistent with this hypothesis, ubiquitination of FADD was reduced and total FADD protein levels were increased in the livers of mice exposed to Gao-binge EtOH feeding in mice.

One limitation of our study is that we have not directly defined a physical interaction between CISH and FADD. CISH is a substrate-recognition component of a stem cell factor–like ECS (elongin B/C-CUL2/5-SOCS-box protein) E3 ubiquitin–protein ligase complex, and is therefore not itself an autonomous E3 ligase.[49] All CISH/SOCS family proteins (CISH, SOCS1, SOCS2, SOCS3, SOCS4, SOCS5, SOCS6, and SOCS7) have a central SH2 domain and a C-terminally located SOCS box.[50] Although the interaction between CISH and FADD could potentially be verified by immunoprecipitation, a large number of additional experiments would still be needed to clarify the functional relationship between CISH and FADD ubiquitination. We plan to further explore this functional relationship in future studies, as they may provide information on therapeutic targets.

Taken together, our study established a miRNA-E3 ligase regulatory network for protein substrates enriched in the programmed cell death pathways and experimentally verified the changes in the key components in this miR-150-5p-CISH-FADD regulatory network in the liver from both patients with AH and a murine model of acute-on-chronic EtOH exposure. Nevertheless, this study has some limitations. First, the sample size of microarray data is relatively small; further studies with larger samples are necessary. Second, while the expression of components in the miRNA-E3 ligase-substrate regulatory network were confirmed experimentally, the mechanism for regulation was not investigated. Given the contribution of

dysregulated control of cell death in the progression of ALD, it will be important for future studies to investigate the complexity of miRNA-E3 ligase regulatory relationships in ALD, to better understand the underlying pathogenesis of ALD.

REFERENCES

1) **Szabo G**, **Kamath PS**, **Shah VH**, **Thursz M**, **Mathurin P**, Addolorato G, et al. Alcohol-related liver disease: areas of consensus, unmet needs and opportunities for further study. Hepatology 2019;69:2271-2283.

2) Crabb DW, Im GY, Szabo G, Mellinger JL, Lucey MR. Diagnosis and treatment of alcohol-associated liver diseases: 2019 practice guidance from the American Association for the Study of Liver Diseases. Hepatology 2020;71:306-333.

3) Louvet A, Thursz MR, Kim DJ, Labreuche J, Atkinson SR, Sidhu SS, et al. Corticosteroids reduce risk of death within 28 days for patients with severe alcoholic hepatitis, compared with pentoxifylline or placebo—a meta-analysis of individual data from controlled trials. Gastroenterology 2018;155:458-468.e458.

4) Zhang Z, Xie G, Liang LI, Liu H, Pan J, Cheng H, et al. RIPK3-mediated necroptosis and neutrophil infiltration are associated with poor prognosis in patients with alcoholic cirrhosis. J Immunol Res 2018;2018:1509851.

5) Wang S, Pacher P, De Lisle RC, Huang H, Ding WX. A mechanistic review of cell death in alcohol-induced liver injury. Alcohol Clin Exp Res 2016;40:1215-1223.

6) Natori S, Rust C, Stadheim LM, Srinivasan A, Burgart LJ, Gores GJ. Hepatocyte apoptosis is a pathologic feature of human alcoholic hepatitis. J Hepatol 2001;34:248-253.

7) Guicciardi ME, Malhi H, Mott JL, Gores GJ. Apoptosis and necrosis in the liver. Compr Physiol 2013;3:977-1010.

8) Tagami A, Ohnishi H, Moriwaki H, Phillips M, Hughes RD. Fas-mediated apoptosis in acute alcoholic hepatitis. Hepatogastroenterology 2003;50:443-448.

9) Taïeb J, Mathurin P, Poynard T, Gougerot-Pocidalo MA, Chollet-Martin S. Raised plasma soluble Fas and Fas-ligand in alcoholic liver disease. Lancet 1998;351:1930-1931.

10) Pastorino JG, Shulga N, Hoek JB. TNF-alpha-induced cell death in ethanol-exposed cells depends on p38 MAPK signaling but is independent of Bid and caspase-8. Am J Physiol Gastrointest Liver Physiol 2003;285:G503-G516.

11) Pritchard MT, Cohen JI, Roychowdhury S, Pratt BT, Nagy LE. Early growth response-1 attenuates liver injury and promotes hepatoprotection after carbon tetrachloride exposure in mice. J Hepatol 2010;53:655-662.

12) **Luedde T**, Kaplowitz N, **Schwabe RF**. Cell death and cell death responses in liver disease: mechanisms and clinical relevance. Gastroenterology 2014;147:765-783.e764.

13) Wertz IE, Dixit VM. Ubiquitin-mediated regulation of TNFR1 signaling. Cytokine Growth Factor Rev 2008;19:313-324.

14) Witt A, Vucic D. Diverse ubiquitin linkages regulate RIP kinases-mediated inflammatory and cell death signaling. Cell Death Differ 2017;24:1160-1171.

15) Wang S, Ni H-M, Dorko K, Kumer SC, Schmitt TM, Nawabi A, et al. Increased hepatic receptor interacting protein kinase 3 expression due to impaired proteasomal functions contributes to alcohol-induced steatosis and liver injury. Oncotarget 2016;7:17681-17698.

16) **Dondelinger Y**, **Darding M**, **Bertrand MJ**, Walczak H. Polyubiquitination in TNFR1-mediated necroptosis. Cell Mol Life Sci 2016;73:2165-2176.

17) Vince JE, **Wong WW**, **Khan N**, **Feltham R**, Chau D, Ahmed AU, et al. IAP antagonists target cIAP1 to induce TNFalpha-dependent apoptosis. Cell 2007;131:682-693.

18) Sadowski M, Sarcevic B. Mechanisms of mono- and poly-ubiquitination: ubiquitination specificity depends on compatibility between the E2 catalytic core and amino acid residues proximal to the lysine. Cell Div 2010;5:19.

19) Lecker SH, Goldberg AL, Mitch WE. Protein degradation by the ubiquitin-proteasome pathway in normal and disease states. J Am Soc Nephrol 2006;17:1807-1819.

20) Fataccioli V, Andraud E, Gentil M, French SW, Rouach H. Effects of chronic ethanol administration on rat liver proteasome activities: relationship with oxidative stress. Hepatology 1999;29:14-20.

21) Donohue TM Jr, Zetterman RK, Zhang-Gouillon ZQ, French SW. Peptidase activities of the multicatalytic protease in rat liver after voluntary and intragastric ethanol administration. Hepatology 1998;28:486-491.

22) Donohue TM Jr. The ubiquitin-proteasome system and its role in ethanol-induced disorders. Addict Biol 2002;7:15-28.

23) Torres JL, Novo-Veleiro I, Manzanedo L, Alvela-Suarez L, Macias R, Laso FJ, et al. Role of microRNAs in alcohol-induced liver disorders and non-alcoholic fatty liver disease. World J Gastroenterol 2018;24:4104-4118.

24) Heo MJ, Kim TH, You JS, Blaya D, Sancho-Bru P, Kim SG. Alcohol dysregulates miR-148a in hepatocytes through FoxO1, facilitating pyroptosis via TXNIP overexpression. Gut 2019;68:708-720.

25) Kim A, Saikia P, Nagy LE. miRNAs involved in M1/M2 hyperpolarization are clustered and coordinately expressed in alcoholic hepatitis. Front Immunol 2019;10:1295.

26) **Chen Z**, **Zhang W**, **Jiang K**, **Chen B**, Wang K, Lao L, et al. MicroRNA-300 regulates the ubiquitination of PTEN through the CRL4B(DCAF13) E3 ligase in osteosarcoma cells. Mol Ther Nucleic Acids 2018;10:254-268.

27) Goto Y, Kojima S, Kurozumi A, Kato M, Okato A, Matsushita R, et al. Regulation of E3 ubiquitin ligase-1 (WWP1) by microRNA-452 inhibits cancer cell migration and invasion in prostate cancer. Br J Cancer 2016;114:1135-1144.

28) Blaya D, Coll M, Rodrigo-Torres D, Vila-Casadesús M, Altamirano J, Llopis M, et al. Integrative microRNA profiling in alcoholic hepatitis reveals a role for microRNA-182 in liver injury and inflammation. Gut 2016;65:1535-1545.

29) Affò S, Dominguez M, Lozano JJ, Sancho-Bru P, Rodrigo-Torres D, Morales-Ibanez O, et al. Transcriptome analysis identifies TNF superfamily receptors as potential therapeutic targets in alcoholic hepatitis. Gut 2013;62:452-460.

30) Langfelder P, Horvath S. WGCNA: an R package for weighted correlation network analysis. BMC Bioinformatics 2008;9:559.

31) Ritchie ME, Phipson B, Wu D, Hu Y, Law CW, Shi W, et al. limma powers differential expression analyses for RNA-sequencing and microarray studies. Nucleic Acids Res 2015;43:e47.

32) Fan Y, Siklenka K, Arora SK, Ribeiro P, Kimmins S, Xia J. miRNet—dissecting miRNA-target interactions and functional associations through network-based visual analysis. Nucleic Acids Res 2016;44:W135-W141.

33) Zhou Y, Zhou B, Pache L, Chang M, Khodabakhshi AH, Tanaseichuk O, et al. Metascape provides a biologist-oriented resource for the analysis of systems-level datasets. Nat Commun 2019;10:1523.

34) Poulsen KL, McMullen MR, Huang E, Kibler CD, Sheehan MM, Leng L, et al. Novel role of macrophage migration inhibitory factor in upstream control of the unfolded protein response after ethanol feeding in mice. Alcohol Clin Exp Res 2019;43:1439-1451.

35) Sanz-Garcia C, Poulsen KL, Bellos D, Wang H, McMullen MR, Li X, et al. The non-transcriptional activity of IRF3 modulates

hepatic immune cell populations in acute-on-chronic ethanol administration in mice. J Hepatol 2019;70:974-984.

36) O'Brien J, Hayder H, Zayed Y, Peng C. Overview of microRNA biogenesis, mechanisms of actions, and circulation. Front Endocrinol (Lausanne) 2018;9:402.

37) **Miyata T**, **Wu XQ**, Fan XD, Huang E, Sanz-Garcia C, Du Ross C, et al. Differential role of MLKL in alcohol-associated and non-alcoholic fatty liver disease in mice and human. JCI insight 2021 (in press).

38) Rennie W, Kanoria S, Liu C, Mallick B, Long D, Wolenc A, et al. STarMirDB: a database of microRNA binding sites. RNA Biol 2016;13:554-560.

39) **Lee EW**, Seo J, Jeong M, **Lee S**, **Song J**. The roles of FADD in extrinsic apoptosis and necroptosis. BMB Rep 2012;45:496-508.

40) Zhuge B, Li G. MiR-150 deficiency ameliorated hepatosteatosis and insulin resistance in nonalcoholic fatty liver disease via targeting CASP8 and FADD-like apoptosis regulator. Biochem Biophys Res Commun 2017;494:687-692.

41) Chen W, Han C, Zhang J, Song K, Wang Y, Wu T. miR-150 deficiency protects against FAS-induced acute liver injury in mice through regulation of AKT. PLoS One 2015;10:e0132734.

42) Chen W, Yan X, Yang A, Xu A, Huang T, You H. miRNA-150-5p promotes hepatic stellate cell proliferation and sensitizes hepatocyte apoptosis during liver fibrosis. Epigenomics 2020;12:53-67.

43) Venugopal SK, Jiang J, Kim T-H, Li Y, Wang S-S, Torok NJ, et al. Liver fibrosis causes downregulation of miRNA-150 and miRNA-194 in hepatic stellate cells, and their overexpression causes decreased stellate cell activation. Am J Physiol Gastrointest Liver Physiol 2010;298:G101-G106.

44) Chen A, Gao B, Zhang J, McEwen T, Ye SQ, Zhang D, et al. The HECT-type E3 ubiquitin ligase AIP2 inhibits activation-induced T-cell death by catalyzing EGR2 ubiquitination. Mol Cell Biol 2009;29:5348-5356.

45) Zeng FC, Zeng MQ, Huang L, Li YL, Gao BM, Chen JJ, et al. Downregulation of VEGFA inhibits proliferation, promotes apoptosis, and suppresses migration and invasion of renal clear cell carcinoma. Onco Targets Ther 2016;9:2131-2141.

46) Duncan SA, Baganizi DR, Sahu R, Singh SR, Dennis VA. SOCS proteins as regulators of inflammatory responses induced by bacterial infections: a review. Front Microbiol 2017;8:2431.

47) Jensik PJ, Arbogast LA. Regulation of cytokine-inducible SH2-containing protein (CIS) by ubiquitination and Elongin B/C interaction. Mol Cell Endocrinol 2015;401:130-141.

48) Holler N, Zaru R, Micheau O, Thome M, Attinger A, Valitutti S, et al. Fas triggers an alternative, caspase-8-independent cell death pathway using the kinase RIP as effector molecule. Nat Immunol 2000;1:489-495.

49) Okumura F, Joo-Okumura A, Nakatsukasa K, Kamura T. The role of cullin 5-containing ubiquitin ligases. Cell Div 2016;11:1.

50) Kile BT, Schulman BA, Alexander WS, Nicola NA, Martin HME, Hilton DJ. The SOCS box: a tale of destruction and degradation. Trends Biochem Sci 2002;27:235-241.

Author names in bold designate shared co-first authorship.

Supporting Information

Additional Supporting Information may be found at onlinelibrary.wiley.com/doi/10.1002/hep4.1677/suppinfo.